

Article

Effectiveness of SO_x, NO_x, and Primary Particulate Matter Control Strategies in the Improvement of Ambient PM Concentration in Taiwan

Jiun-Horng Tsai ^{1,2}, Ming-Ye Lee ¹ and Hung-Lung Chiang ^{3,*}

¹ Department of Environmental Engineering, National Cheng Kung University, Tainan 701, Taiwan; jhtsai@ncku.edu.tw (J.-H.T.); cceq10502myl@gmail.com (M.-Y.L.)

² Research Center for Climate Change and Environment Quality, National Cheng Kung University, Tainan 701, Taiwan

³ Department of Safety Health and Environmental Engineering, National Yunlin University of Science and Technology, Yunlin 64002, Taiwan

* Correspondence: hlchiang@yuntech.edu.tw; Tel.: +886-5-536-1489; Fax: +886-5-536-1353

Abstract: The Community Multiscale Air Quality (CMAQ) measurement was employed for evaluating the effectiveness of fine particulate matter control strategies in Taiwan. There are three scenarios as follows: (I) the 2014 baseline year emission, (II) 2020 emissions reduced via the Clean Air Act (CAA), and (III) other emissions reduced stringently via the Clean Air Act. Based on the Taiwan Emission Data System (TEDs) 8.1, established in 2014, the emission of particulate matter 2.5 (PM_{2.5}) was 73.5 thousand tons y⁻¹, that of SO_x was 121.3 thousand tons y⁻¹, and that of NO_x was 404.4 thousand tons y⁻¹ in Taiwan. The CMAQ model simulation indicated that the PM_{2.5} concentration was 21.9 μg m⁻³. This could be underestimated by 24% in comparison with data from the ambient air quality monitoring stations of the Taiwan Environmental Protection Administration (TEPA). The results of the simulation of the PM_{2.5} concentration showed high PM_{2.5} concentrations in central and southwestern Taiwan, especially in Taichung and Kaohsiung. Compared to scenario I, the average annual concentrations of PM_{2.5} for scenario II and scenario III showed reductions of 20.1% and 28.8%, respectively. From the results derived from the simulation, it can be seen that control of NO_x emissions may improve daily airborne PM_{2.5} concentrations in Taiwan significantly and control of directly emitted PM_{2.5} emissions may improve airborne PM_{2.5} concentrations each month. Nevertheless, the results reveal that the preliminary control plan could not achieve the air quality standard. Therefore, the efficacy and effectiveness of the control measures must be considered to better reduce emissions in the future.

Keywords: Community Multiscale Air Quality (CMAQ); SO_x; NO_x; sulfate; nitrate; primary particulate matter



Citation: Tsai, J.-H.; Lee, M.-Y.; Chiang, H.-L. Effectiveness of SO_x, NO_x, and Primary Particulate Matter Control Strategies in the Improvement of Ambient PM Concentration in Taiwan. *Atmosphere* **2021**, *12*, 460. <https://doi.org/10.3390/atmos12040460>

Academic Editors: Soontae Kim and Rafael Borge

Received: 3 March 2021

Accepted: 31 March 2021

Published: 6 April 2021

Publisher's Note: MDPI stays neutral with regard to jurisdictional claims in published maps and institutional affiliations.



Copyright: © 2021 by the authors. Licensee MDPI, Basel, Switzerland. This article is an open access article distributed under the terms and conditions of the Creative Commons Attribution (CC BY) license (<https://creativecommons.org/licenses/by/4.0/>).

1. Introduction

Air pollutants have a significant influence on global human health, quality of life, premature deaths and mortality rate, and the occurrence of different respiratory illnesses related to ambient air quality [1–6]. Each year, approximately seven million premature deaths are recorded across the world. Specifically, one-eighth of the total deaths in the world are due to the combined effects of household and ambient air pollution [7]. Air pollution causes considerable economic impacts and also increases medical expenses, and the related loss of working days reduces economic productivity [8]. In Asia, it is estimated that about 7% of the gross domestic product (GDP) loss was attributed to local air pollution [9]. As far as the health risks associated with this particulate matter are concerned, many epidemiological studies have been published to understand associated cardiovascular diseases, respiratory diseases, cancer, and birth defects [10–17]. Moreover, a few studies have found a link between particles and inflammatory responses in sensitive

people [18–20]. As discussed above, the influence of particulate matter (PM) on human health is considered a crucial factor for air quality management.

Particulate matter (PM) pollution, which shortens the lives of humans significantly, contributes to a wide range of diseases [21,22]. Many epidemiological studies have identified a positive correlation associating cardiovascular diseases, respiratory disease, and PM [10,23,24]. In addition, studies have indicated that PM is closely related to increases in the mortality rates of lung cancer and other cardiopulmonary diseases [25–27]. Fine atmospheric aerosol mass concentrations are detrimental due to their influence on the respiratory system, their impact on visibility conditions, and their role in global climate change [28,29]. In addition, to carbonaceous species, sulfate, nitrate, and ammonium are the major species present in fine particulate matter in most situations [29]. In a study by Dongarrà et al. [30], water-soluble ions consisted of a large fraction of PM₁₀ and PM_{2.5} and ammonium, sulfate, and nitrate particles accounted for 14–29% of the PM mass concentration. In the European population, the prevalence of the secondary inorganic aerosol (SIA) could be twice as high as that of the primary fine particulate matter [31]. In a Danish cohort study, the results indicated that long-term exposure to PM_{2.5}, black carbon/organic carbon (BC/OC), and secondary organic aerosols causes cardiovascular disease and mortality [32]. Therefore, the formation of the secondary aerosol fraction could be essential for understanding the source of fine PM contribution and set up PM control strategies. Furthermore, gas-phase reactions, such as SO₂ and NO₂, are precursors to the production of H₂SO₄ and HNO₃ via photochemical reactions, and this makes it possible for them to transfer into particulate matter [33]. Behera and Sharma [34] investigated the degradation of SO₂, NO₂, and NH₃, and they found that these could form secondary inorganic aerosols in an environmental chamber study. Secondary inorganic particulate matter, the dominant component of fine particles, is formed by homogeneous and heterogeneous reactions among gas species [35–37].

In addition, the effectiveness of air pollution control strategies is assessed to improve ambient air quality, reduce exposure, and support human health. The US Environmental Protection Agency (EPA) [38] is following the Clean Air Act (CAA) to use quality models for the assessment of regulations, control strategies, and actions to not only reduce emissions but also improve ambient air quality. Air dispersion models are considered important to inform a number of different regulatory assessments, e.g., the Regulatory Impact Assessments, used to guide federal actions, and the National Ambient Air Quality Standards (NAAQS), used to assess hazardous air pollutants and other health and ecosystem measures. In Europe, the control of air pollutant emissions and related regulations were enacted with the intention to improve air quality across Europe [8]. In recent years, the Community Multiscale Air Quality (CMAQ) model has been implemented with comprehensive halogen sources and chemistry [39] to examine the overall influence of halogen species on air pollution over Europe, as the grid size can affect the predictions of the CMAQ model [40]. Some research studies have been performed in northeastern U.S., including urban health impact studies using the Community Multiscale Air Quality (CMAQ) models to determine air pollution exposure. Results indicate that a larger domain is highly recommended for summer and weekends in eastern U.S. [41].

The observations at these stations can only monitor the level of pollutants around particular locations. However, the emission, transport, and transformation of pollution over the whole region can be shown by these models. Therefore, it is essential to harmonize the criteria with capable and competent models to reproduce air quality features over a particular region in order to officially report national air pollution levels and examine compliance with regulations [6].

In China, about one million deaths per year are attributed to air pollution [42]. The Air Pollution Prevention and Control Action Plan (APPCAP) was implemented to reduce PM_{2.5} concentration from 2013 to 2017, and the results indicated a 6.8% reduction rate in mortality attributable to PM_{2.5} pollution in 2017 compared to that in 2013. This supports the effectiveness of the APPCAP [42]. The question of how to validate the effectiveness

of air pollution control strategies could be an important focus for future works on air quality management.

In Taiwan, some studies have indicated that the CMAQ simulation is associated with a dynamic NH_3 emissions approach that could improve diurnal and seasonal variations and reduce simulation bias [43]. A real-time air quality forecasting (AQF) system was developed using the Weather Research and Forecasting meteorological model and the CMAQ model for $\text{PM}_{2.5}$ prediction, and the AQF system was able to reduce the $\text{PM}_{2.5}$ forecast error and improve the root-mean-square error (RMSE) and mean bias (MB) calculations [44]. In addition, local sources could be the most important emission sources and the emissions of the power plants and iron/steel industries were under control. The management of motor vehicle emissions and construction/road dust should be taken into consideration to improve $\text{PM}_{2.5}$ levels in Taiwan [45].

Over the past decade, $\text{PM}_{2.5}$ concentrations have presented a decreasing trend, as determined by the Taiwan EPA monitoring station network. The average concentration was $34 \mu\text{g m}^{-3}$ in 2007 and $30 \mu\text{g m}^{-3}$ in 2013. However, it still exceeds the level of $15 \mu\text{g m}^{-3}$ (the annual average concentration) set by Taiwan's National Ambient Air Quality Standard (NAAQS). Therefore, the effectiveness of air pollution control strategies is important to enforce an emission reduction in gas precursors such as SO_x and NO_x and primary particulate matter for improvement in ambient air quality.

The objective of this study was improvement in ambient $\text{PM}_{2.5}$ concentrations using various control measures under different scenarios. Emissions of primary $\text{PM}_{2.5}$, SO_x , and NO_x were estimated, and an air quality model, CMAQ, was employed in simulating the ambient concentration of $\text{PM}_{2.5}$. The simulated concentrations of each scenario were compared to those generated from basic cases to demonstrate the effectiveness of the $\text{PM}_{2.5}$ control measures.

2. Materials and Methods

2.1. Model Simulation

The US Environmental Protection Agency's Community Multiscale Air Quality (CMAQ) modeling system version 4.7.1, associated with the fifth-generation Pennsylvania State University National Center for Atmospheric Research Mesoscale Model (MM5) version 3.7, was adopted to simulate ambient concentrations of $\text{PM}_{2.5}$ in Taiwan. The modeling system took into account the chemistry and physics of pollutant transport, as presented in the guidelines suggested by Byun and Schere [46] and simultaneous frameworks proposed by Wong et al. [47]. The system consists of three-level nested domains, as shown in Figure 1, where domain 1 (D1) covers east and south Asia ($81 \text{ km} \times 81 \text{ km}$), domain 2 (D2) covers Mainland China and east Asia (Japan and Korea) ($27 \text{ km} \times 27 \text{ km}$), and domain 3 (D3) covers southeast China and Taiwan ($9 \text{ km} \times 9 \text{ km}$).

Meteorology outputs were processed with the Meteorology–Chemistry Interface Processor (MCIP) [48] (version 4.3). The purpose was to build air-quality-model-ready meteorological input files.

CMAQ default profiles were used for the 81km outermost domain's lateral boundary conditions (BCs) and initial conditions (ICs). Boundary conditions for finer domains are normally generated from coarser domains. Using ICON (Initial condition) and BCON (Boundary condition) modules, part of the preprocessing of the modules of CMAQ involved the preparation BCs and ICs. The CMAQ Chemistry-Transport Model (CCTM) with a Euler Backward Iterative (EBI) chemistry solver for photochemical mechanisms was used. The chemical mechanism used for the gaseous species was the carbon bond mechanism (CB05) [49].

There are many methods and performance indicators to validate the model simulation. Generally, the performance of a dispersion model simulation can be assessed by the mean fractional error (MFE) ($\leq \pm 50\%$) and the mean fractional bias (MFB) ($\leq \pm 30\%$), and extended diagnostic evaluation and sensitivity tests can improve the performance of the model simulation [50–52]. Results of the model simulation are used for a relative rather than

an absolute prediction for the selection of effective control strategies and determination of the uncertainty associated with model predictions [51].

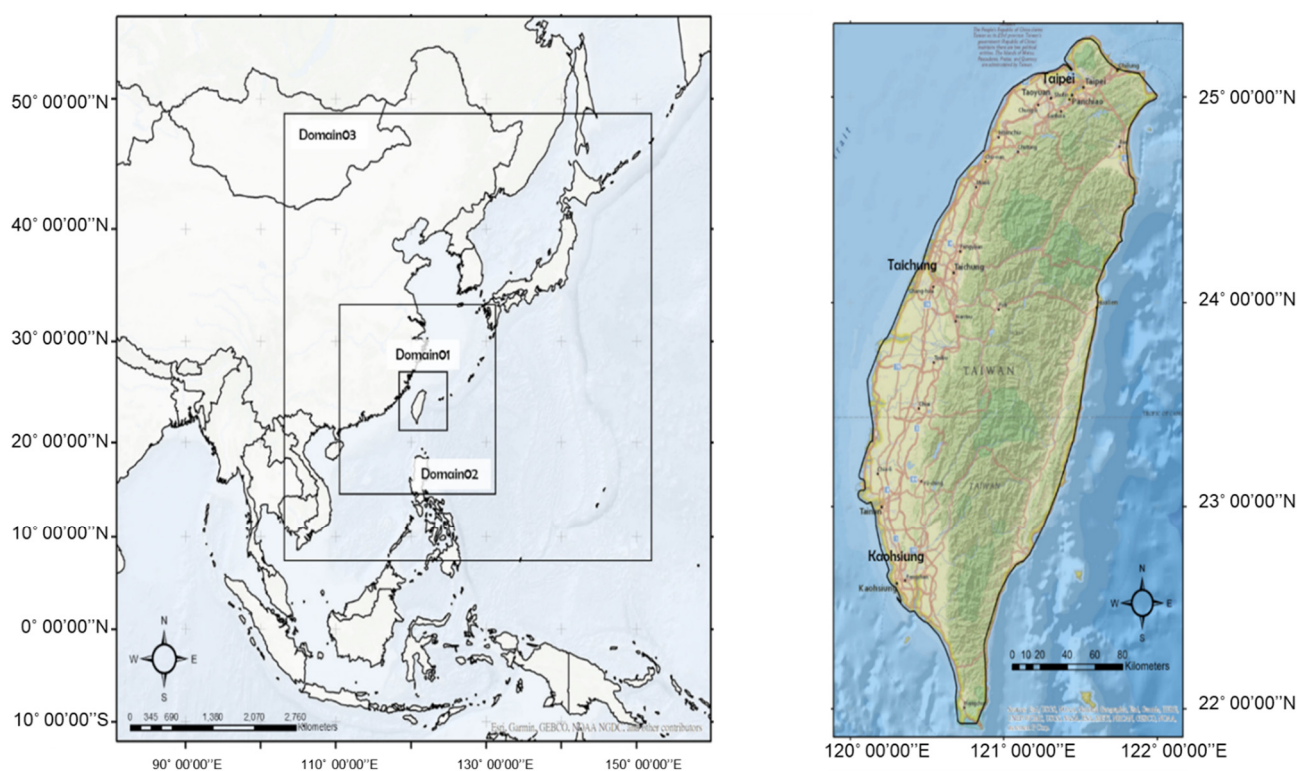


Figure 1. The simulation domain and setting.

The forecasting of the PM concentration is important for air quality management; however, the work focused on the effectiveness of control strategies. The 9 km grid resolution could be coarse for ambient air quality forecasting; the resolution could be enough to evaluate the performance of control measures relevant to this work. More high-resolution simulations can be prepared for future work.

Some indicators were selected to evaluate the performance of the MM5. The average results indicated the MBE (Mean bias error) ($0.2\text{ }^{\circ}\text{C}$) and MAGE (Mean absolute gross error) ($1.7\text{ }^{\circ}\text{C}$) for temperature, MBE (2.4 m s^{-1}) and RMSE (Root Mean Square Error) (3.7 m s^{-1}) for wind speed, and the WNMB (Wind normalized mean bias) (-5.3%) and WNME (Wind normalized mean error) (29.7%) for wind direction. In the research statement, the wind speed was deemed an overestimation that could be one of the reasons for the underestimation of the $\text{PM}_{2.5}$ concentration in this work compared with that of the monitoring stations.

For the model simulation, the MFE and MFB were selected for $\text{PM}_{2.5}$ performance. Results indicated that the MFB and MFE were -0.48 (from -0.33 to -0.68) and 0.77 (from 0.69 to 0.88), respectively. The indices of MFE and MFB were out of the criteria of model simulation performance: $\text{MFB} \leq \pm 0.30$ and $\text{MFE} \leq \pm 0.50$ [51]. The emission database, complex topography, and overestimation of wind speed (results of the MM5) could be the important reasons to lead the $\text{PM}_{2.5}$ simulation out of criteria.

2.2. Emission

The Sparse Matrix Operator Kernel Emissions (SMOKE) model was developed to use matrix–vector multiplication for efficient emission processing. The SMOKE modeling system commonly used to calculate emissions for regional CMAQ applications has recently been fine-tuned to support hemispheric CMAQ applications to allow for more streamlined implementation of the various emission processing steps described above [53].

The emission data used 1 km × 1 km data from the Taiwan Emission Data System (TEDs) v8.1 by referring to the format of SMOKE. The monitoring concentrations from the Taiwan Environmental Protection Administration (TEPA) air quality monitoring station were included here to evaluate model performance.

2.3. Scenarios

In this study, emission scenarios consisting of three parts were evaluated: a basic case and two controlled cases. The basic case, scenario I, represented the emissions from stationary sources and mobile sources and fugitive emissions in the base year (2014) following the emission standards of TEDs 8.1 developed and proven by TEPA. It focused on permitted emissions from stationary sources, showing emission conditions in 2014. The other scenarios were based on TEDs 8.1 and reduced the air pollution emissions following the control strategies of the different scenarios in 2020. According to the contents of the control measures, the emissions of primary PM_{2.5}, e.g., sulfur dioxide (SO_x) and nitrogen dioxide (NO_x), under different scenarios were estimated. Scenario II was an adapted plan (Taiwan Clean Air Act Plan) designed to include more stringent emission standards for stationary sources (especially power plants) and on-road mobile sources, eliminate high-polluting aged vehicles, and promote electric vehicles. For scenario III, it was assumed that more control measures could be conducted beyond scenario II. The measures involved included the elimination of two-stroke motorcycles, the promotion of hybrid vehicles and electric buses, and encouragement of the use of natural gas in power plants (shown in Table 1).

Table 1. The control strategies of the different scenarios.

Scenario	Strategies
Scenario I Year–2014	Baseline year–2014
Scenario II Taiwan Clean Air Act (TCAA) 2020	<ul style="list-style-type: none"> • Allow emission growth by demand. • Power plant: replace the generation sector. • Conduct the state implement plan. • Make stringent the emission standards for power plants. • Identify mobile sources. • Replace two-stroke motorcycles. • Replace old buses. • Fugitive source: control river dust.
Scenario III TCAA and implement more control strategies Year–2020	<ul style="list-style-type: none"> • Follow the strategies of scenario II. • Implement more control strategies. • Make stringent the emission standards of existing sources (power plants; basic iron and steel manufacturing; petroleum and coal product manufacturing; chemical material manufacturing; petrochemical manufacturing; pulp, paper, and paper product manufacturing; and others). • Phase out two-stroke motorcycles. • Promote clean fuels. ◆ Promote liquefied natural gas (LNG) for power plants. ◆ Promote use of hybrid oil–electricity passenger cars. ◆ Electrify buses.

3. Results and Discussion

3.1. Baseline Conditions: Scenario I

The emissions of SO_x, NO_x, and PM_{2.5} were 121.3, 404.5, and 73.5 thousand tons per year, respectively, for scenario I. The emission distributions of PM_{2.5}, SO_x, and NO_x are illustrated in Figure 2. SO_x were mainly emitted from stationary sources (a fraction of 90% from stationary sources, 36% from power plants, 14% from the iron and steel industry, and

9% from the manufacture of chemical materials) (shown as Figure 3). A total of 90% of NOx was attributed to stationary sources and mobile sources; heavy-duty diesel vehicles (20%), power plants (18%), gasoline passenger cars (8%), diesel buses (6%), and the manufacture of chemical materials (5%) were considered dominant sources (shown as Figure 4). The most abundant PM_{2.5} emissions were from fugitive emissions (such as cooking fumes from restaurants (10%), construction engineering (6%), and agricultural burning (6%)), mobile source emissions (11% from motor vehicles, 6% from gasoline passenger cars, and 6% from heavy-duty diesel vehicles), and stationary sources (the iron and steel industry and power plants), as shown in Figure 5.

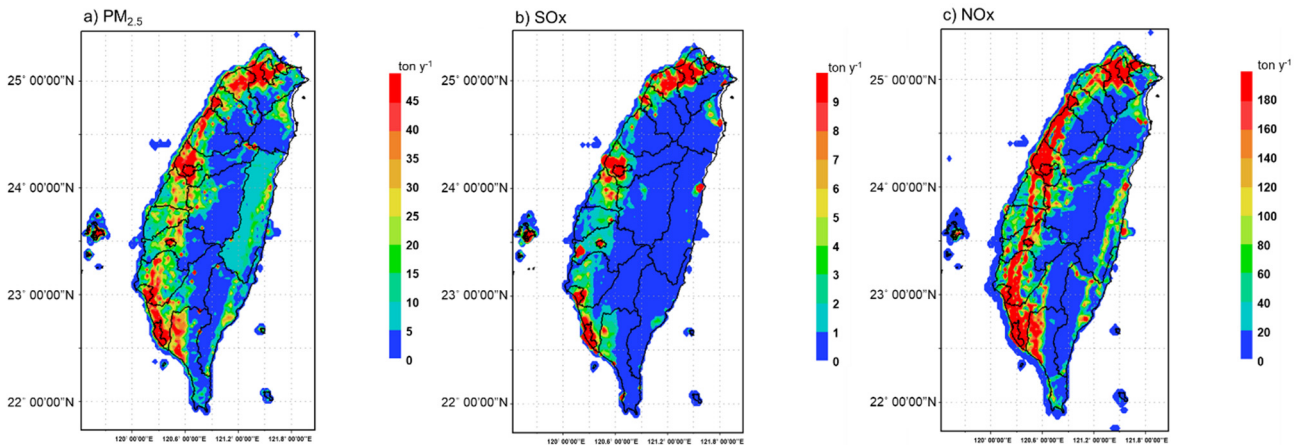
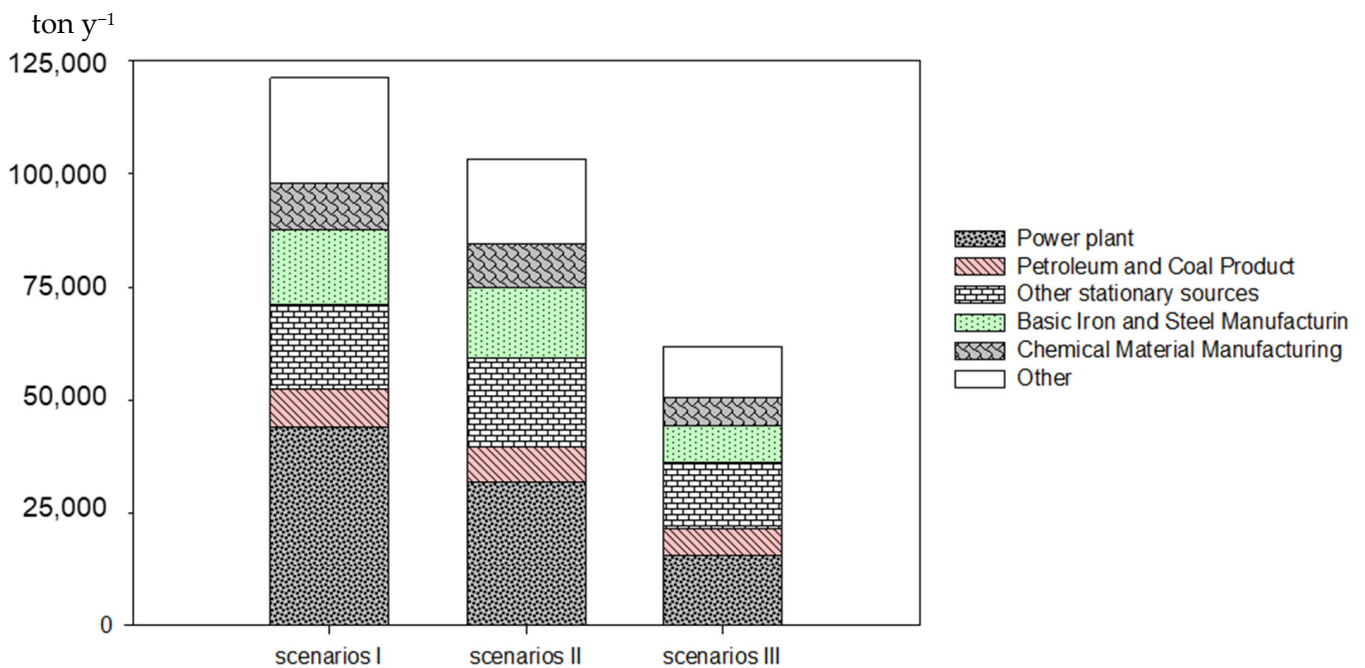
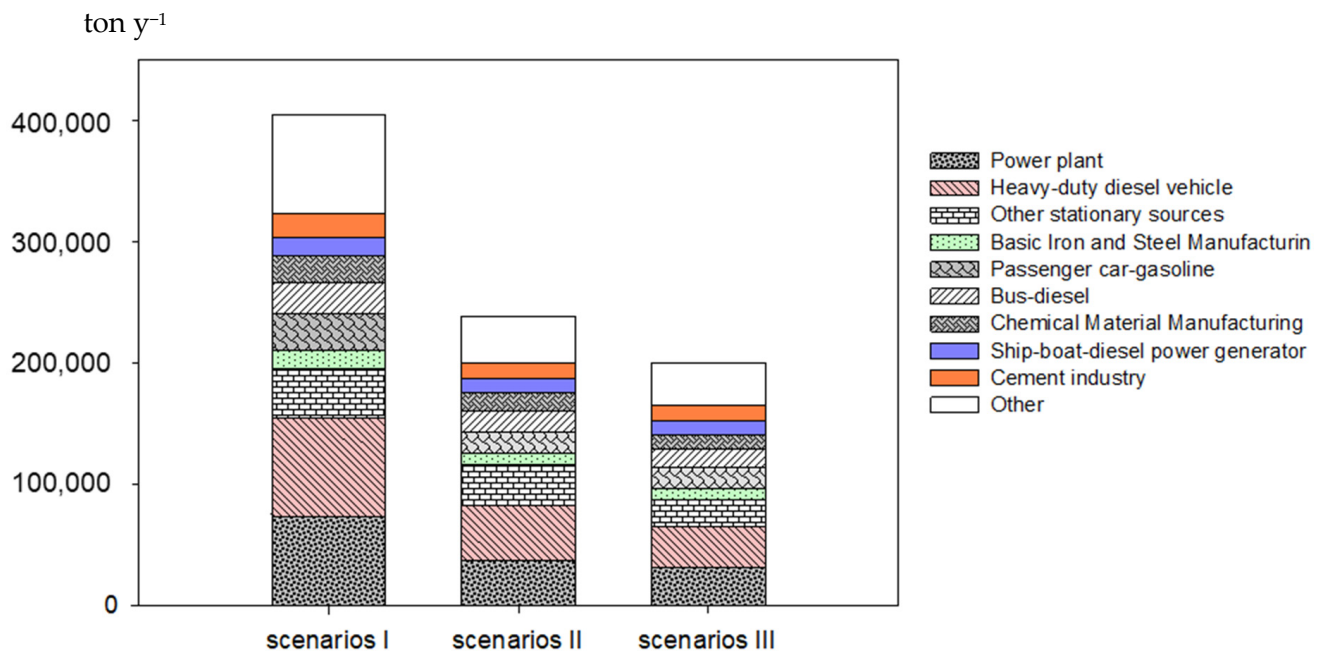


Figure 2. The emission distribution (ton y⁻¹) of PM_{2.5} (a), SOx (b), and NOx (c) in the baseline year (scenario I).



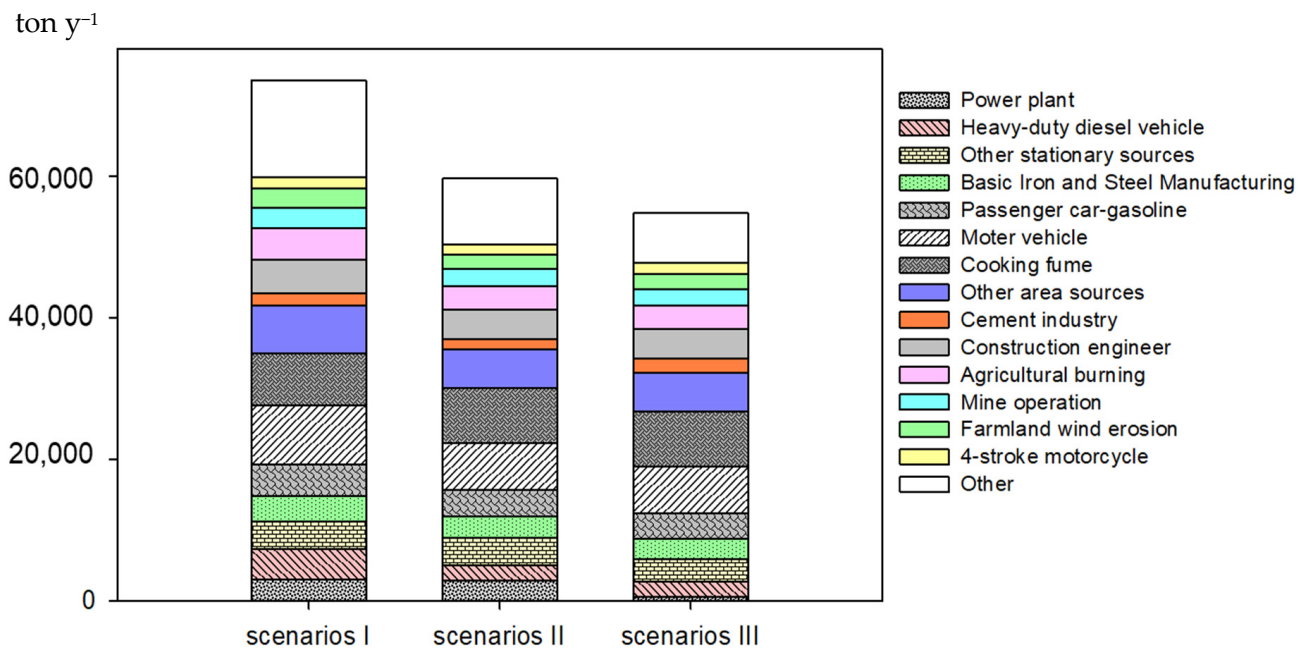
Other* : Ship-boat-diesel Power Generator, Petrochemicals Manufacturing, Pulp, Paper and Paper Products Manufacturing, Commercial Combustion-heavy Oil, Other Area Sources, Ship and Boat Combustion-diesel, Agriculture Burning, Passenger car-gasoline, Ship and Boat Combustion-heavy Oil, Heavy-duty Diesel Vehicle, 4-stroke Motorcycle, 2-stroke Motorcycle, Light Duty Gasoline Vehicle, Business Passenger Car-gasoline, Bus-diesel, Light-duty Diesel Vehicle, Bus, Passenger Car-diesel

Figure 3. SO₂ emission sources for different scenarios (ton y⁻¹).



Other* : 4-stroke Motorcycle, Petrochemicals Manufacturing, Bus, Petroleum and Coal Products Manufacturing, Light Duty Gasoline Vehicle, Other Area Sources, Agriculture Burning, Business Passenger Car-gasoline, Light-duty Diesel Vehicle, 2-stroke Motorcycle, Commercial Combustion-heavy Oil, Aircraft Combustion Emission, Ship and Boat Combustion-diesel, Passenger Car-diesel, Passenger Car -LPG, Commercial Combustion-diesel

Figure 4. NOx emission sources for different scenarios (ton y⁻¹).



Other* : Chemical Material Manufacturing, Non-metallic Mineral Products Manufacturing, Bus-diesel, River Fugitive Dust, Farming, Light Duty Gasoline Vehicle, Metallic Mineral Products Manufacturing, Petrochemicals Manufacturing, Light-duty Diesel Vehicle, Business Passenger Car-gasoline, Bus, Pulp, Paper and Paper Products Manufacturing, Motor Vehicle (Non-paved road), Mining, Petroleum and Coal Products, Manufacturing, Passenger Car-diesel, Ship-boat-diesel Power Generator, Ship-boat-diesel, Passenger Car-LPG, 2-stroke motorcycle

Figure 5. PM_{2.5} emission sources for different scenarios (ton y⁻¹).

SOx emission distributions were mainly concentrated in urban and industrial complex areas and harbors. NOx emissions were in the urban areas of western Taiwan, and transportation activities involving the use of freeways and highways were the main sources of NOx emissions. PM_{2.5} emissions were abundant in the urban areas of western Taiwan, where activities of transportation take place, as given in Figure 2.

The annual average concentration of PM_{2.5} was 21.9 $\mu\text{g m}^{-3}$ after the CMAQ simulation; there was a 24% underestimation in comparison with the average monitoring data derived from the Taiwan EPA air quality monitoring stations in 2014, as depicted in Figure 6. The MFB and MFE did not meet the criteria, which could be important reasons for the underestimation of the PM simulation. The model simulation did not clearly determine high-PM episodes, especial in January, which was a limitation of the application of the model to predict the ambient air quality. PM concentration forecasting is important for air quality management; however, the study evaluated the effectiveness of control strategies under different scenarios.

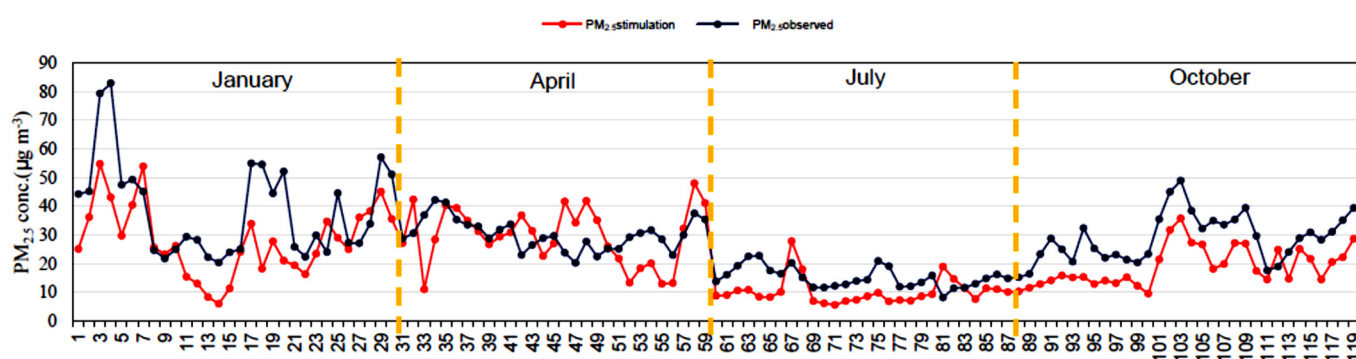


Figure 6. The modeling simulation of PM_{2.5} concentrations ($\mu\text{g m}^{-3}$) of the ambient air quality monitoring stations.

In addition, this work discussed SOx and NOx reactions and their transfer into particulate matter. However, we do not believe that NH₃ and the secondary organic aerosol come from photochemical reactions. According to the literature, the total mass of sulfate, nitrate, and ammonium constituted 39.9–44.3% of the PM_{2.5} mass [54] in southern Taiwan, and the mass fractions of secondary organic matter in PM_{2.5} were estimated to be 14–22% [55]. Over 50% of the mass of fine particulate matter came from the chemical reactions required to form secondary PM_{2.5}. The overestimation of wind speed and chemical reactions did not include NH₃ and the secondary organic aerosol, which could explain the underestimation of ambient PM_{2.5} concentrations.

The monthly average PM_{2.5} simulation concentrations were in the order 29.7 $\mu\text{g m}^{-3}$ (April) > 28.0 $\mu\text{g m}^{-3}$ (January) > 19.7 $\mu\text{g m}^{-3}$ (October) > 10.3 $\mu\text{g m}^{-3}$ (July). Relatively high PM_{2.5} concentrations were observed in central and southern Taiwan, as presented in Figure 7. Moreover, relatively high PM concentrations were determined in April, and the same data were also collected from TEPAir monitoring stations. Therefore, the PM concentration was observed to be high in winter and spring. In contrast, the PM concentration was low in summer. That was because the rainy season is from May to September and sometimes can last until October or November.

Primary PM_{2.5}, known as directly emitted PM, is the dominant fraction of the total PM_{2.5}. The concentrations of nitrate were higher than those of sulfate in central and southern Taiwan in January, April, and October, as described in Figure S1. Based on the model simulation and statistical analysis, results of the correlation between PM_{2.5} and the composition of airborne PM_{2.5} showed that the PM_{2.5} concentrations were closely related to nitrate ($r = 0.93$), primary PM_{2.5}, ($r = 0.80$), and sulfate ($r = 0.70$), with a strong correlation ($r > 0.7$).

According to the emissions of the baseline year, high sulfate concentrations were located in the southwest region and the highest abundant concentrations were observed in April, as can be seen in Figure S2. A rather high nitrate concentration was found in central

and southern Taiwan. In addition, in January, the highest average nitrate concentration was found around the Kaoping air basin, located in southwestern Taiwan (Figure S3). Primary $PM_{2.5}$ was high in central and southwestern Taiwan. The highest concentration period was observed in January, especially in the southwestern area of Taiwan.

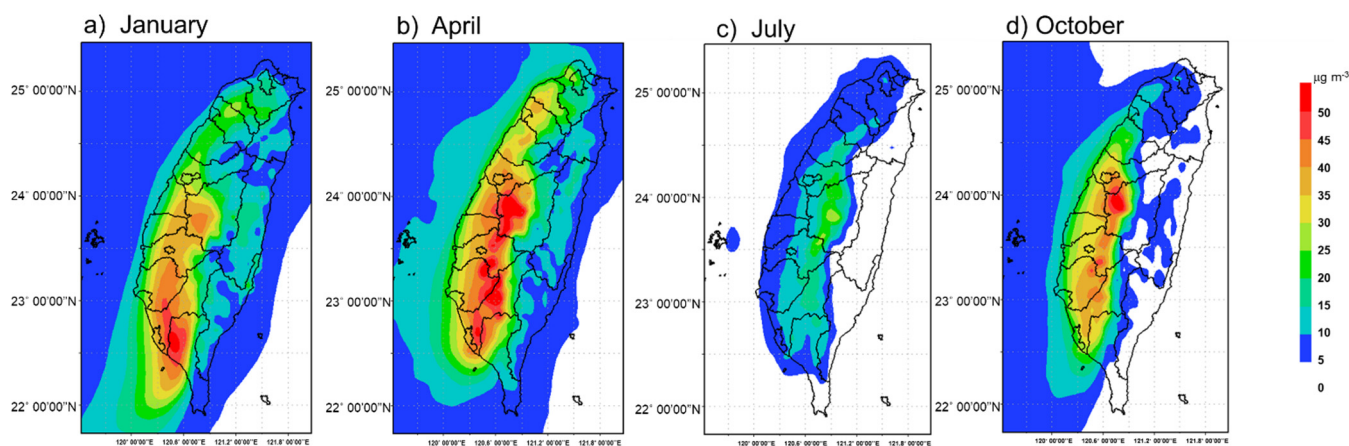


Figure 7. $PM_{2.5}$ concentration ($\mu\text{g m}^{-3}$) simulations for January (a), April (b), July (c), and October (d) under baseline year conditions.

According to the model simulation, primary $PM_{2.5}$ was found to contribute 20–40% of the mass of the total $PM_{2.5}$. High primary $PM_{2.5}$ contributions were found to be in the northern and central parts of western Taiwan. The nitrate mass fraction tended to increase in the seasons with high levels of PM mass, especially in January and April, in central and southwestern Taiwan.

3.2. Scenario II: The Taiwan Clean Air Act (TCAA) Plan Adopted

The reduction in SO_x was 17.9 thousand tons per year, and the reduction in NO_x was 158 thousand tons per year. In addition, the reduction in $PM_{2.5}$ emissions was 13.9 thousand tons per year. For scenario II, the emissions of SO_x , NO_x , and $PM_{2.5}$ were 103.4, 246.3, and 59.7 thousand tons per year, respectively, as shown in Figure 8.

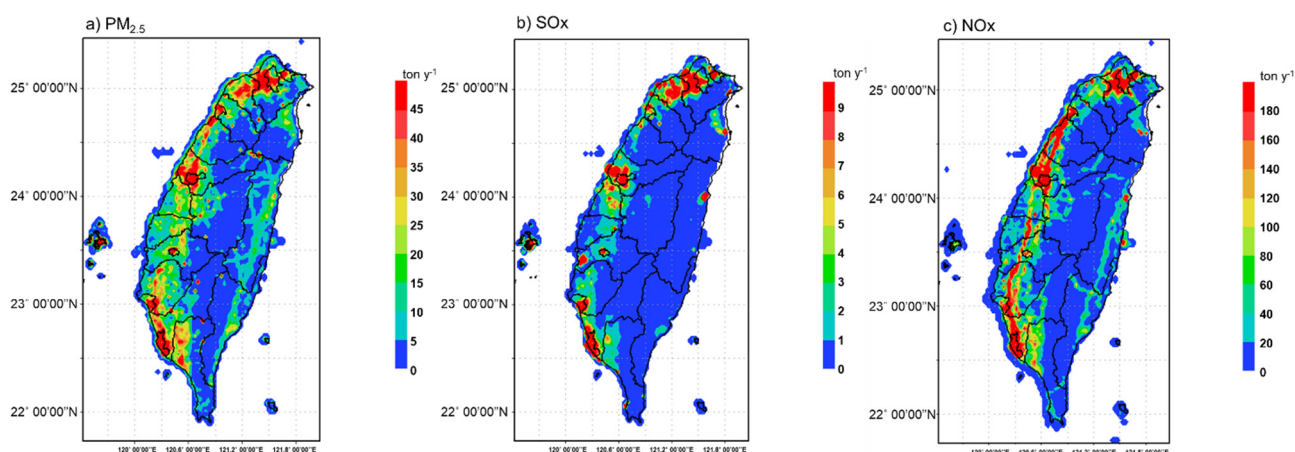


Figure 8. The emission distribution (ton y^{-1}) of $PM_{2.5}$ (a), SO_x (b), and NO_x (c) for scenario II.

The SO_x reductions were mainly from changes in power plants (the installation of new electricity-generating units and change of fuels from coal or heavy oil to liquefied natural gases). The emission of 12 thousand tons was attributed to changes in basic iron

and steel production, 1.1 thousand tons to the manufacture of chemical materials, and 0.7 thousand tons to other sources, as depicted in Figure 3 for scenario II.

NO_x reduction via power plants was 73 thousand tons per year, via heavy-duty diesel vehicles was 43 thousand tons per year, via gasoline passenger cars was 14 thousand tons per year, and via buses powered by diesel was 13 thousand tons per year (shown as Figure 4, scenario II).

Considering different emission sources, the PM_{2.5} concentration could be reduced. The major reduction came from the following human activities and motor vehicles: (1) heavy-duty diesel vehicles, 2.1 thousand tons per year; (2) motor vehicle driving, 1.7 thousand tons per year; (3) agricultural burning, 1.1 thousand tons per year; (4) passenger cargasoline, 1.1 thousand tons per year; and (5) two-stroke motorcycles, 1.0 thousand tons per year, as illustrated in Figure 5, scenario II.

The monthly average PM_{2.5} simulation concentrations of scenario II were shown as Figure 9.

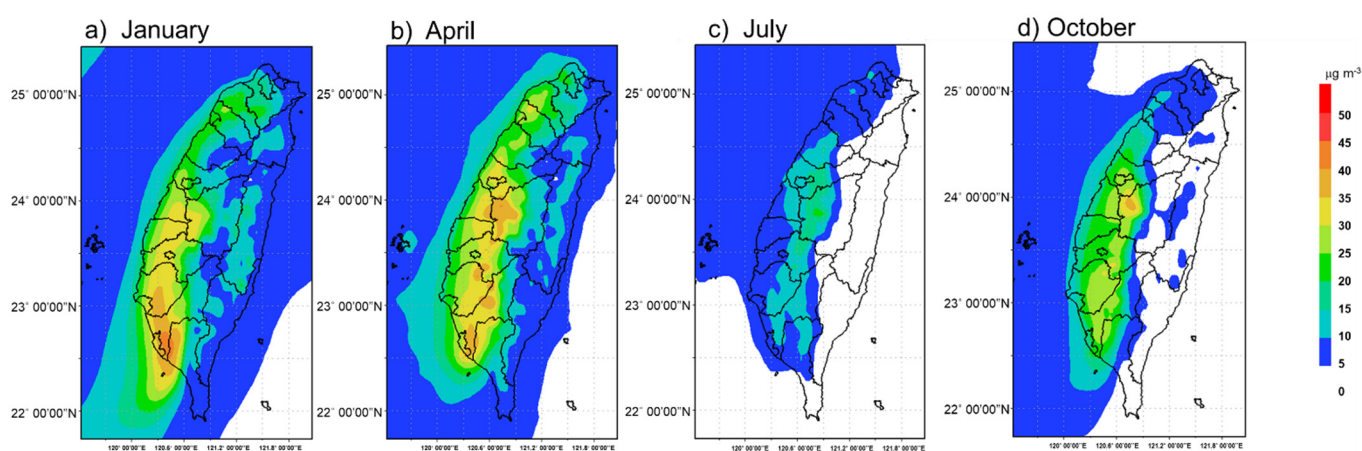


Figure 9. PM_{2.5} concentration ($\mu\text{g m}^{-3}$) simulations for January (a), April (b), July (c), and October (d) under scenario II.

Primary PM_{2.5} concentrations increased from northwestern ($2.8\text{--}5.2 \mu\text{g m}^{-3}$) to southwestern ($3.4\text{--}9.6 \mu\text{g m}^{-3}$) Taiwan. The highest concentration was determined in southwestern Taiwan in January. In east Taiwan, the primary PM concentration was $0.8\text{--}2.6 \mu\text{g m}^{-3}$, as described in Figure S4.

Regarding the sulfate concentration distribution, high sulfate concentrations were determined in southern Taiwan and their concentration could be over $2.5 \mu\text{g m}^{-3}$ in January. The sulfate concentration was also high in central Taiwan ($2.1 \mu\text{g m}^{-3}$). In April, the sulfate concentration inland was higher than that near the seaside areas in central Taiwan. The sulfate concentrations were $2.1\text{--}2.8 \mu\text{g m}^{-3}$ in western areas and $1.4\text{--}1.5 \mu\text{g m}^{-3}$ in eastern areas. In July, the sulfate concentration was reduced to half of the concentration observed in January and April. After the rainy season, the concentration increased to $1.1\text{--}2.1 \mu\text{g m}^{-3}$ in the west and $0.9\text{--}1.0 \mu\text{g m}^{-3}$ in western Taiwan in October, as shown in Figure S5.

Nitrate concentrations were high (January: $1.4\text{--}7.1 \mu\text{g m}^{-3}$; April: $1.5\text{--}4.7 \mu\text{g m}^{-3}$; July: $0.2\text{--}0.7 \mu\text{g m}^{-3}$; October: $0.2\text{--}3.6 \mu\text{g m}^{-3}$) in western Taiwan, especially southwestern Taiwan ($0.4\text{--}7.1 \mu\text{g m}^{-3}$). Lower concentrations ($0.00\text{--}0.7 \mu\text{g m}^{-3}$) were found in July due to the rainy season in this period. In east Taiwan, the nitrate concentrations were within the range of $0.0\text{--}0.4 \mu\text{g m}^{-3}$, as presented in Figure S6.

State and local governments have planned to eliminate older two-stroke motorcycles and older buses and control the fugitive dust emissions from the river. The annual average concentration of PM_{2.5} in scenario II was $17.5 \mu\text{g m}^{-3}$. There was a 20.1% concentration reduction in ambient PM_{2.5} between scenarios I and II. The monthly average reductions in PM_{2.5} concentrations were 18.3% in October, 17.2% in April, 14.4% in January, and 14.3% in July. High PM_{2.5} concentration reduction was observed in central and southern Taiwan, as shown in Figure S2a. Primary PM_{2.5} is still the dominant component. The

results of the correlation between $PM_{2.5}$ and the composition of airborne $PM_{2.5}$ proved the $PM_{2.5}$ concentration to be related to nitrate ($r = 0.92$), primary $PM_{2.5}$ ($r = 0.82$), and sulfate ($r = 0.76$).

In January, the primary $PM_{2.5}$ mass fractions were 28–38% for different air basins. The sulfate mass in $PM_{2.5}$ fractions (9.1–24%) was higher than that observed in both northern and eastern Taiwan. High nitrate mass fractions were determined in central (16%) and southern (18%) Taiwan. In April, primary $PM_{2.5}$ mass fractions were 22–32%, the sulfate fraction was 12–24%, and the nitrate fraction was 1.2–12%. A low PM mass was observed in July. The primary PM and sulfate mass fractions were found to be increasing, and a decrease in the nitrate fraction could be attributed to the rainy season in July, as nitrate compounds easily dissolve and react under high-moisture conditions. In October, the PM and sulfate fractions decreased and the nitrate fraction increased instead.

3.3. Scenario III: Conducted TCCA and More Control Strategies

The reduction in SO_x was 59.5 thousand tons per year, NO_x was reduced to 200 thousand tons per year, and $PM_{2.5}$ reduction was 18.8 thousand tons per year when compared with the emissions of scenario I. The emissions of SO_x , NO_x , and $PM_{2.5}$ were 61.8, 204.7, and 54.8 thousand tons per year, respectively, for scenario III, as shown in Figure 10. The differences of emissions between scenarios II and III are shown in Figure S7. The reductions were mainly because of phasing out two-stroke motorcycles, promoting electric motor vehicles and buses in downtown, and increasing liquefied natural gas (LNG) consumption at power plants.

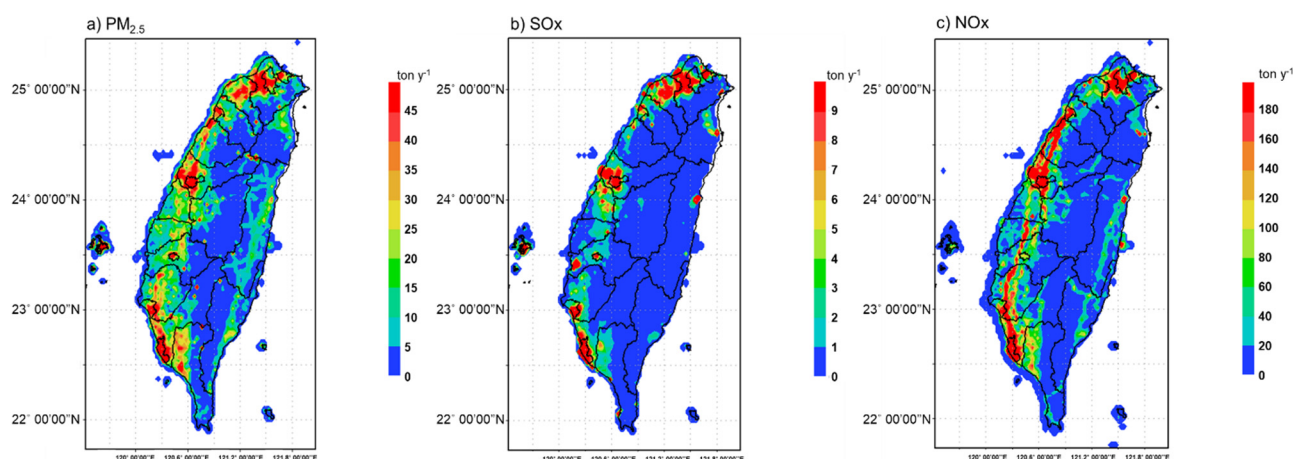


Figure 10. The emission distribution (ton y^{-1}) of $PM_{2.5}$, SO_x , and NO_x for scenario III.

For scenario III, the control strategies followed those adopted in scenario II and more strategies and control measures for SO_x and NO_x such as the phasing out of two-stroke motorcycles, the clean fuel program (liquefied natural gas (LNG) is used in power plants), and the electric bus program were included, as given in Figures 3 and 4, scenario III).

SO_x reductions were mainly from LNG application in power plants (a reduction of 31.7 thousand tons per year), and reductions from other categories were less than 1.5 thousand tons per year.

NO_x reductions were mainly from power plants and electric buses. The former contributed 24 thousand tons per year. The latter contributed 4.0 thousand tons per year. Chemical material manufacturing also contributed 2.2 thousand tons per year, and the cement industry contributed 3.3 thousand tons per year.

The monthly average $PM_{2.5}$ simulation concentrations of scenario III were shown as Figure 11.

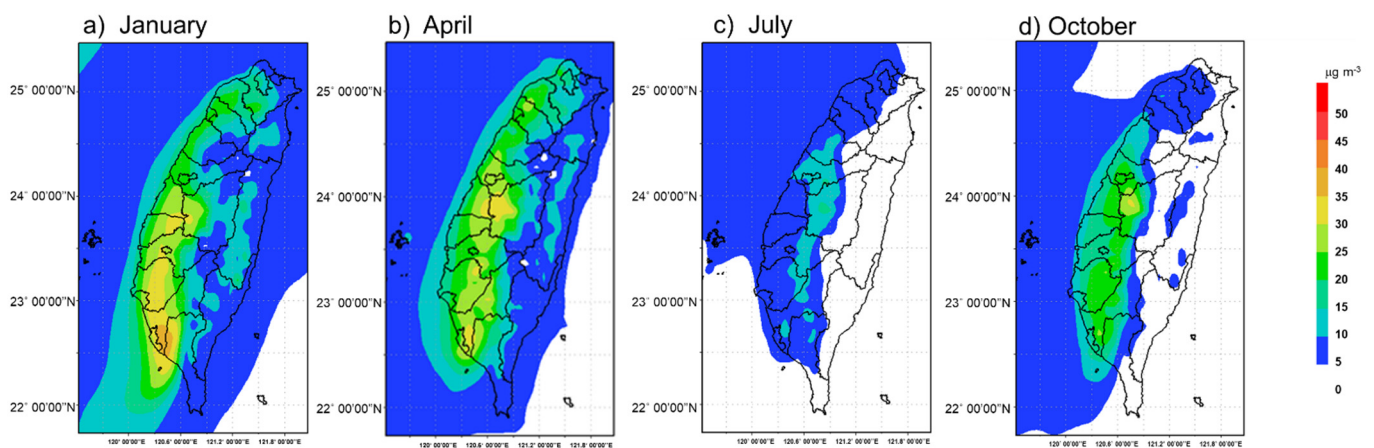


Figure 11. PM_{2.5} concentration ($\mu\text{g m}^{-3}$) simulations for January (a), April (b), July (c), and October (d) under scenario III.

As to the primary PM_{2.5} distribution ($0.8\text{--}9.2 \mu\text{g m}^{-3}$), the results indicated that high PM_{2.5} concentrations were observed in southern ($3.2\text{--}9.2 \mu\text{g m}^{-3}$) and central ($3.2\text{--}7.5 \mu\text{g m}^{-3}$) Taiwan. The highest primary PM_{2.5} concentration was about $10 \mu\text{g m}^{-3}$ in southern Taiwan in January. Low PM_{2.5} concentrations ($0.8\text{--}3.2 \mu\text{g m}^{-3}$) were determined in July. (shown as Figure S8).

PM_{2.5} emissions were reduced via power plants (a reduction of 2.8 thousand tons per year), and the sulfate concentration distribution was $0.7\text{--}2.3 \mu\text{g m}^{-3}$. The results indicated the highest sulfate concentration ($1.1\text{--}2.3 \mu\text{g m}^{-3}$) in southern Taiwan. There was a relatively high sulfate concentration ($1.3\text{--}2.1 \mu\text{g m}^{-3}$) in central Taiwan in comparison with that in north Taiwan ($1.1\text{--}1.9 \mu\text{g m}^{-3}$) and that in east Taiwan ($0.7\text{--}1.4 \mu\text{g m}^{-3}$). The months of January ($1.4\text{--}2.2 \mu\text{g m}^{-3}$), October ($0.9\text{--}1.8 \mu\text{g m}^{-3}$), and April ($1.4\text{--}2.3 \mu\text{g m}^{-3}$) presented relatively high sulfate levels, with relatively low ones in July ($0.7\text{--}1.3 \mu\text{g m}^{-3}$) due to the rainy season from May to September in Taiwan, as illustrated in Figure S9.

In terms of the nitrate concentration distribution ($0\text{--}6.2 \mu\text{g m}^{-3}$), high concentrations ($0.3\text{--}6.2 \mu\text{g m}^{-3}$) were observed in southern Taiwan. High nitrate concentrations were found in central Taiwan in April. In July, the nitrate concentrations were less than $0.5 \mu\text{g m}^{-3}$ because of the rainy season in Taiwan (shown as Figure S10).

The annual average concentration of PM_{2.5} for scenario III was $17.5 \mu\text{g m}^{-3}$. Compared with the basic case in 2014, the simulated concentration was reduced by 28.8%. The monthly average PM_{2.5} concentration reductions were 10.5% (April), 10.0% (October), 8.6% (July), and 5.5% (January), sequentially. A significant reduction in the PM_{2.5} concentration was also observed in central and southern Taiwan, as described in Figure 11.

In January, sulfate concentrations were within the range of $1.7\text{--}2.2 \mu\text{g m}^{-3}$ in western Taiwan and a high-abundance area was located in southwestern Taiwan. High nitrate concentrations were located in central and southwestern Taiwan, and the concentration range was $4.1\text{--}6.2 \mu\text{g m}^{-3}$ (nitrate fraction of PM_{2.5} was 15–17%). The primary PM_{2.5} concentration ranged from 7.5 to $9.2 \mu\text{g m}^{-3}$ (the fraction was 31.3–38.6%), and the corresponding areas were from the central part of Taiwan to the southwestern part of Taiwan. In the western part of Taiwan, the PM concentration increased from the northern area to the southern area.

In April, sulfate concentrations were $1.9\text{--}2.3 \mu\text{g m}^{-3}$, and these were slightly increased in comparison with those observed in January in the same area. For nitrate, the concentrations were within the range of $3.3\text{--}3.8 \mu\text{g m}^{-3}$ (the nitrate fraction of PM_{2.5} was 10–11%) in western Taiwan. High primary PM_{2.5} levels were located at central (concentration: $5.6 \mu\text{g m}^{-3}$) and southern (concentration: $5.7 \mu\text{g m}^{-3}$) Taiwan. In July, a high sulfate concentration was in the central air basin, and its concentration was $1.3 \mu\text{g m}^{-3}$. In addition, the concentration of nitrate was high ($1.5 \mu\text{g m}^{-3}$) as well in the air basin. The primary PM concentration was about $3.2 \mu\text{g m}^{-3}$ in the central and southern air basins. Sulfate ($1.5\text{--}1.8 \mu\text{g m}^{-3}$), nitrate ($2.0\text{--}2.7 \mu\text{g m}^{-3}$, a fraction representing 7.9–11% of the PM

mass), and primary PM concentrations increased in October compared with those observed in July.

3.4. Effectiveness of Pollutant Reductions

Three major emission types consisting of NO_x, SO_x, and directly emitted PM_{2.5} were determined to contribute to the ambient PM_{2.5} aerosol mass. The implemented control strategies of the air quality management program (AQMP) help reduce SO_x, NO_x, and direct PM_{2.5} emissions substantially. As presented earlier, the trends in SO_x, NO_x, and PM_{2.5} emissions suggest a direct relationship between lower emissions and improvements in air quality.

In scenario II, it was shown that replacement of older power plants could be an effective strategy for reducing directly emitted PM, SO_x, and NO_x. In addition, the replacement of old heavy-duty diesel vehicles could reduce NO_x and PM emissions, as shown in Figures 3–5.

In scenario III, SO₂ emission reductions were mainly from the use of clean fuel (LNG) in power plants, basic iron and steel manufacturing, chemical material manufacturing, and petroleum and coal product manufacturing. NO_x reductions were from the use of LNG in power plants, the phasing out of heavy-duty diesel vehicles, and the replacement of diesel buses with electric buses. LNG power plants, vehicle phase-outs, exhaust control devices, and the retrofitting of old heavy-duty diesel vehicles could be relatively effective control strategies for reducing PM emissions in scenario III.

It is useful to evaluate the relative value of the ambient microgram per cubic meter improvements in ambient PM_{2.5} under the per ton precursor emission reductions. Table 2 presents the relative contributions of precursor emission reductions to ambient PM_{2.5} concentrations in scenario II and scenario III. The analysis determines that SO_x emission reductions had the lowest return in terms of micrograms per cubic meter on the per ton emissions of PM_{2.5} reductions, about half that of NO_x reductions. NO_x emission reductions were about twice as effective as SO_x emission reductions for ambient PM_{2.5} concentration reduction. However, the reductions in directly emitted PM_{2.5} emissions were approximately 14–19 times more effective than SO_x emission reductions. The results of scenarios II and III indicated that the sequence of the effectiveness of PM_{2.5} concentration reduction was primary PM_{2.5} > NO_x > SO_x.

Table 2. Relative contributions of precursor emission reductions of the simulated PM_{2.5} concentration.

Precursor	PM Fraction	Scenario II	Scenario III
SO _x	Sulfate	1	1
NO _x	Nitrate	2.1	1.7
PM _{2.5}	Primary PM _{2.5}	19	14

4. Conclusions

A simulated high PM_{2.5} concentration of the baseline scenario was observed in central and southern Taiwan. The period with the higher PM level was found to range from October to April of the following year. This was because the rainy season is from May to September in Taiwan. Directly emitted PM_{2.5} was found to be the major component of total PM_{2.5}. Nitrate was considered a higher fraction of the PM_{2.5} mass than sulfate in high-PM_{2.5}-concentration areas and periods. There was also a relatively high correlation between simulated PM_{2.5} concentration and nitrate during high-PM-concentration periods. The emission reduction rates of scenario II and scenario III were 20.1% and 28.8%, respectively, in comparison with the rate of scenario I. The replacement of antiquated power plants and the use of clean LNG fuel, the replacement of old motor vehicles, and stringent emission standards for stationary sources could be effective strategies for not only reducing emissions but also improving ambient air quality. However, the reduction in emissions by enactment of the Taiwan Clean Air Act Plan and enhanced control measures is still unable to achieve the annual average PM_{2.5} standard of 15 µg m⁻³. SO₂ emission reduction

might help improve ambient air PM_{2.5}. In addition, the relative contribution of precursor emission reductions to PM_{2.5} suggests that NO_x emission control could lessen the problem of high PM_{2.5} concentrations and primary PM_{2.5} emission control might improve ambient PM_{2.5} concentrations in Taiwan, regardless of time and space. For the simulation in this work, the metrics of the MFE and MFB could not meet the criteria of model performance. The modeling system can be updated to more recent versions, which could be one of the routes to improving its simulation performance benchmarks.

Supplementary Materials: The following are available online at <https://www.mdpi.com/article/10.3390/atmos12040460/s1>, Figure S1: The stimulation of primary PM_{2.5} concentrations for January (a), April (b), July (c) and October (d) under the baseline year condition, Figure S2: The stimulation of sulfate concentrations for January (a), April (b), July (c) and October (d) under the baseline year condition, Figure S3: The stimulation of nitrate concentrations for January (a), April (b), July (c) and October (d) under the baseline year condition, Figure S4: The stimulation of primary PM_{2.5} concentrations for January (a), April (b), July (c) and October (d) under Scenario II, Figure S5: The stimulation of sulfate concentrations for January (a), April (b), July (c) and October (d) under the scenario II, Figure S6: The stimulation of nitrate concentrations for January (a), April (b), July (c) and October (d) under Scenario II, Figure S7: The stimulation of Primary PM_{2.5} concentrations for January (a), April (b), July (c) and October (d) under the scenario III, Figure S8: The stimulation of sulfate concentrations for January (a), April (b), July (c) and October (d) under the scenario III, Figure S9: The stimulation of Nitrate concentrations for January (a), April (b), July (c) and October (d) under the scenario III, Figure S10: Comparison the differences of Scenario II (Figure 5) and III (Figure 6). (a) PM_{2.5}; (b) Sox; (c) NO_x.

Author Contributions: Conceived and designed the study, J.-H.T.; analyzed the data and model stimulation, M.-Y.L., H.-L.C., and J.-H.T.; wrote and revised the paper, H.-L.C. and J.-H.T. All authors have read and agreed to the published version of the manuscript.

Funding: This research was supported by the Ministry of Science and Technology, Taiwan.

Institutional Review Board Statement: Not applicable.

Informed Consent Statement: Not applicable.

Data Availability Statement: All the data are present in the manuscript.

Acknowledgments: The authors express their sincere thanks to the Ministry of Science and Technology, Executive Yuan, Republic of China (Taiwan), for research fund support (MOST 101-2221-E-006-160-MY3 and MOST 104-2221-E-006-020-MY3).

Conflicts of Interest: The authors declare no conflict of interest.

References

1. Giannadaki, D.; Pozzer, A.; Lelieveld, J. Modeled global effects of airborne desert dust on air quality and premature mortality. *Atmos. Chem. Phys.* **2014**, *14*, 957–968. [[CrossRef](#)]
2. Lelieveld, J.; Hadjinicolaou, P.; Kostopoulou, E.; Giannakopoulos, C.; Tanarhte, M.; Tyrlis, E. Model projected heat extremes and air pollution in the Eastern Mediterranean and Middle East in the twenty-first century. *Reg. Environ. Chang.* **2014**, *14*, 1937–1949. [[CrossRef](#)]
3. Abdo, N.; Khader, Y.S.; Abdelrahman, M.; Graboski-Bauer, A.; Malkawi, M.; Al-Sharif, M.; Elbetieha, A.M. Respiratory health outcomes and air pollution in the Eastern Mediterranean region: A systematic review. *Rev. Environ. Health* **2016**, *31*, 259–280. [[CrossRef](#)] [[PubMed](#)]
4. Khader, Y.S.; Abdo, N.; Abdelrahman, M.; Al-Sharif, M.; Bateiha, A.M.; Malkawi, M. The effect of air pollution on cancer in the Eastern Mediterranean region: A systematic literature review. *J. Environ. Pollut. Hum. Health* **2016**, *4*, 66–71.
5. Dayan, U.; Ricaud, P.; Zinder, R.; Dulac, F. Atmospheric pollution over the eastern Mediterranean during summer—A review. *Atmos. Chem. Phys.* **2017**, *17*, 13233–13263. [[CrossRef](#)]
6. Kushta, J.; Georgiou, G.K.; Proestos, Y.; Christoudias, T.; Thunis, P.; Savvides, C.; Papadopoulos, C.; Lelieveld, J. Evaluation of EU air quality standards through modeling and the FAIRMODE benchmarking methodology. *Air Qual. Atmos. Health* **2019**, *12*, 73–86. [[CrossRef](#)]
7. WHO; Regional Office for Europe; OECD. *Economic Cost of the Health Impact of Air Pollution in Europe: Clean Air, Health and Wealth*; Regional Office for Europe: Copenhagen, Denmark; WHO: Geneva, Switzerland, 2015.
8. EEA (European Environmental Agency). *Air Quality in Europe—2018 Report*; 12/2018; EEA: Luxembourg, 2018; p. 83. [[CrossRef](#)]

9. The World Bank. *The Cost of Air Pollution: Strengthening the Economic Case for Action*; The World Bank: Washington, DC, USA, 2016.
10. Health Effects Institute (HEI). *Revised Analyses of the National Morbidity, Mortality and Air Pollution Study, Part II: Revised Analyses of Selected Time-Series Studies of Air Pollution and Health*; Health Effects Institute: Cambridge, MA, USA, 2003.
11. Cohen, A.J.; Brauer, M.; Burnett, R.; Anderson, H.R.; Frostad, J.; Estep, K.; Balakrishnan, K.; Brunekreef, B.; Dandona, L.; Dandona, R.; et al. Estimates and 25-year trends of the global burden of disease attributable to ambient air pollution: An analysis of data from the Global Burden of Diseases Study. *Lancet* **2017**, *389*, 1907–1918. [[CrossRef](#)]
12. WHO. *Review of Evidence on Health Aspects of Air Pollution-REVIHAAP Project*; Final Technical Report; The WHO European Centre for Environment and Health: Bonn, Switzerland, 2013.
13. Zhou, Y.; Li, L.; Hu, L. Correlation analysis of PM₁₀ and the incidence of lung cancer in Nanchang, China. *Int. J. Environ. Res. Public Health* **2017**, *14*, 1253. [[CrossRef](#)]
14. Burnett, R.T.; Cakmak, S.; Brook, J.R.; Krewski, D. The role of particulate size and chemistry in the association between summertime ambient air pollution and hospitalization for cardiorespiratory disease. *Environ. Health Perspect.* **1997**, *105*, 614–620. [[CrossRef](#)]
15. Ostro, B.D.; Broadwin, R.; Lipsett, M.J. Coarse and fine particles and daily mortality in the Coachella Valley, California: A follow-up study. *J. Expo. Anal. Environ. Epidemiol.* **2000**, *10*, 412–419. [[CrossRef](#)]
16. Brunekreef, B.; Forsberg, B. Epidemiological evidence of effects of coarse airborne particles on health. *Eur. Resp. J.* **2005**, *26*, 309–318. [[CrossRef](#)] [[PubMed](#)]
17. Kan, H.; London, S.J.; Chen, G.; Zhang, Y.; Song, G.; Zhao, N.; Jiang, L.; Chen, B. Differentiating the effects of fine and coarse particles on daily mortality in Shanghai, China. *Environ. Int.* **2007**, *33*, 376–384. [[CrossRef](#)] [[PubMed](#)]
18. Lipsett, M.J.; Tsai, F.C.; Roger, L.; Woo, M.; Ostro, B.D. Coarse particles and heart rate variability among older adults with coronary artery disease in the Coachella Valley, California. *Environ. Health Perspect.* **2006**, *114*, 1215–1220. [[CrossRef](#)] [[PubMed](#)]
19. Hapoo, M.S.; Salonen, R.O.; Hölinen, A.I.; Jalava, P.I.; Pennanen, A.S.; Kosma, V.M.; Sillanpää, M.; Hillamo, R.; Brunekreef, B.; Katsouyanni, K.; et al. Dose and time dependency of inflammatory responses in the mouse lung to urban air coarse, fine, and ultrafine particles from six European cities. *Inhal. Toxicol.* **2007**, *19*, 227–246. [[CrossRef](#)] [[PubMed](#)]
20. Yeatts, K.; Svendsen, E.; Creason, J.; Alexis, N.; Herbst, M.; Scott, J.; Kupper, L.; Williams, R.; Neas, L.; Cascio, W.; et al. Coarse particulate matter (PM_{2.5-10}) affects heart rate variability, blood lipids, and circulating eosinophils in adults with asthma. *Environ. Health Perspect.* **2007**, *115*, 709–714. [[CrossRef](#)]
21. World Health Organization (WHO). *Health Risks of Particulate Matter from Long-Range Transboundary Air Pollution*; World Health Organization: Copenhagen, Denmark, 2006.
22. Pope, C.A., III; Majid, E.; Dogulas, D.W. Fine-particulate air pollution and life expectancy in the United States. *N. Engl. J. Med.* **2009**, *360*, 376–386. [[CrossRef](#)]
23. Oberdorster, G.; Gelein, R.M.; Ferin, J.; Weiss, B. Association of particulate air pollution and acute mortality: Involvement of ultra-fine particles? *Inhal. Toxicol.* **1995**, *7*, 111–124. [[CrossRef](#)]
24. Pope, C.A., III; Dockery, D.W. Health effects of fine particulate air pollution: Lines that connect. *J. Air Waste Manag. Assoc.* **2006**, *56*, 709–742. [[CrossRef](#)]
25. Naess, O.; Piro, F.N.; Nafstad, P.; Smith, G.D.; Leyland, A.H. Air pollution, social deprivation and mortality: A multilevel cohort study. *Epidemiology* **2007**, *18*, 686–694. [[CrossRef](#)]
26. Brunekreef, B.; Beelen, R.; Hoek, G.; Schouten, L.; Bausch-Goldbohm, S.; Fischer, P.; Armstrong, B.; Hughes, E.; Jerrett, M.; van den Brandt, P. *Effects of Long-Term Exposure to Traffic-Related Air Pollution on Respiratory and Cardiovascular Mortality in The Netherlands: The NLCS-AIR Study*; Research Report Health Effects Institute: Boston, MA, USA, 2009; pp. 5–71.
27. Boldo, E.; Linares, C.; Lumbreras, J.; Borge, R.; Narros, A.; García-Pérez, J.; Fernández-Navarro, P.; Pérez-Gómez, B.; Aragonés, N.; Ramis, R.; et al. Health impact assessment of a reduction in ambient PM_{2.5} levels in Spain. *Environ. Int.* **2011**, *37*, 342–348. [[CrossRef](#)]
28. Đorđević, D.; Mihajlidi-Zelić, A.; Relić, D.; Ignjatović, L.J.; Huremović, J.; Stortini, A.M.; Gambaro, A. Size-segregated mass concentration and water soluble inorganic ions in an urban aerosol of the central Balkans (Belgrade). *Atmos. Environ.* **2012**, *46*, 309–317. [[CrossRef](#)]
29. Galindo, N.; Yubero, E.; Clemente, Á.; Nicolás, J.F.; Varea, M.; Crespo, J. PM events and changes in the chemical composition of urban aerosols: A case study in the western Mediterranean. *Chemosphere* **2020**, *244*, 125520. [[CrossRef](#)]
30. Dongarrà, G.; Manno, E.; Varrica, D.; Lombardo, M.; Vultaggio, M. Study on ambient concentrations of PM₁₀, PM_{10-2.5}, PM_{2.5} and gaseous pollutants. Trace elements and chemical speciation of atmospheric particulates. *Atmos. Environ.* **2010**, *44*, 5244–5257. [[CrossRef](#)]
31. Andersson, C.; Bergstro, R.; Johansson, C. Population exposure and mortality due to regional background PM in Europe—Long-term simulations of source region and shipping contributions. *Atmos. Environ.* **2009**, *43*, 3614–3620. [[CrossRef](#)]
32. Hvidtfeldt, U.A.; Geels, C.; Sorensen, M.; Ketzel, M.; Khan, J.; Tjønneland, A.; Christensen, J.H.; Brandt, J.; Raaschou-Nielsen, O. Long-term residential exposure to PM_{2.5} constituents and mortality in a Danish cohort. *Environ. Int.* **2019**, *133*, 105268. [[CrossRef](#)] [[PubMed](#)]
33. Foltescu, V.L.; Selin Lindgern, E.; Isakson, J.; Öblad, M.; Pacyna, J.M.; Benson, S. Gas-to-particle conversion of sulfur and nitrogen compounds as studied at marine stations in northern European. *Atmos. Environ.* **1996**, *30*, 3129–3140. [[CrossRef](#)]

34. Behera, S.N.; Sharma, M. Degradation of SO₂, NO₂ and NH₃ leading to formation of secondary inorganic aerosols: An environmental chamber study. *Atmos. Environ.* **2011**, *45*, 4015–4024. [CrossRef]
35. Gen, M.; Zhang, R.; Huang, D.D.; Li, Y.; Chan, C.K. Heterogeneous SO₂ oxidation in sulfate formation by photolysis of particulate nitrate. *Environ. Sci. Technol. Lett.* **2019**, *6*, 86–91. [CrossRef]
36. Meidan, D.; Holloway, J.S.; Edwards, P.M.; Dubé, W.P.; Middlebrook, A.M.; Liao, J.; Welti, A.; Graus, M.; Warneke, C.; Ryerson, T.B.; et al. Role of cregee intermediates in secondary sulfate aerosol formation in nocturnal power plant plumes in the Southeast US. *ACS Earth Space Chem.* **2019**, *3*, 748–759. [CrossRef]
37. Yang, J.; Li, L.; Wang, S.; Li, H.; Francisco, J.S.; Zeng, X.C.; Gao, Y. Unraveling a new chemical mechanism of missing sulfate formation in aerosol haze: Gaseous NO₂ with aqueous HSO₃⁻/SO₃²⁻. *J. Am. Chem. Soc.* **2021**. [CrossRef]
38. US EPA. Available online: <https://www.epa.gov/cmaq/modeling-toxic-air-pollutants-cmaq> (accessed on 5 April 2020).
39. Sarwar, G.; Gantt, B.; Foley, K.; Fahey, K.; Spero, T.L.; Kang, D.; Mathur, R.; Hosein, F.; Xing, J.; Sherwin, T.; et al. Influence of bromine and iodine chemistry on annual, seasonal, diurnal, and background ozone: CMAQ simulations over the Northern Hemisphere. *Atmos. Environ.* **2019**, *213*, 395–404. [CrossRef]
40. Sommariva, R.; Hollis, L.D.J.; Sherwen, T.; Baker, A.R.; Ball, S.M.; Bandy, B.J.; Bell, T.G.; Chowdhury, M.N.; Cordell, R.L.; Evans, M.J.; et al. Seasonal and geographical variability of nitryl chloride and its precursors in Northern Europe. *Atmos. Sci. Lett.* **2018**, *19*, 844. [CrossRef]
41. Jang, X.; Yoo, E.H. evaluating the effect of domain size of the community multiscale air quality (cmaq) model on regional PM_{2.5} simulations. In *Global Perspectives on Health Geography*; Lu, Y., Delmelle, E., Eds.; Springer Nature: Geneva, Switzerland, 2020.
42. Yue, H.; He, C.; Huang, Q.; Yin, D.; Bryan, B.A. Stronger policy required to substantially reduce deaths from PM_{2.5} pollution in China. *Nat. Commun.* **2020**, *11*, 1462. [CrossRef]
43. Hsu, C.H.; Cheng, F.Y.; Chang, H.Y.; Lin, N.H. Implementation of a dynamical NH₃ emissions parameterization in CMAQ for improving PM_{2.5} simulation in Taiwan. *Atmos. Environ.* **2019**, *218*, 116923. [CrossRef]
44. Cheng, F.Y.; Feng, C.Y.; Yang, Z.M.; Hsu, C.H.; Chan, K.W.; Lee, C.Y.; Chang, S.C. Evaluation of real-time PM_{2.5} forecasts with the WRF-CMAQ modeling system and weather-pattern-dependent bias-adjusted PM_{2.5} forecasts in Taiwan. *Atmos. Environ.* **2021**, *244*, 117909. [CrossRef]
45. Chen, T.F.; Chang, K.H.; Lee, C.H. Simulation and analysis of causes of a haze episode by combining CMAQ-IPR and brute force source sensitivity method. *Atmos. Environ.* **2019**, *218*, 117006. [CrossRef]
46. Byun, D.W.; Schere, K.L. Review of the governing equations, computational algorithms, and other components of the models-3 Community Multiscale Air Quality (CMAQ) modeling system. *Appl. Mech. Rev.* **2006**, *59*, 51–77. [CrossRef]
47. Wong, D.C.; Pleim, J.; Mathur, R.; Binkowski, F.; Otte, T.; Gilliam, R. WRF-CMAQ two-way coupled system with aerosol feedback: Software development and preliminary results. *Geosci. Model Dev.* **2012**, *5*, 299–312. [CrossRef]
48. Otte, T.L.; Pleim, J.E. The Meteorology-Chemistry Interface Processor (MCIP) for the CMAQ modeling system: Updates through MCIPv3.4.1. *Geosci. Model Dev.* **2010**, *3*, 243–256. [CrossRef]
49. Yarwood, G.; Rao, S.; Yocke, M.; Whitten, G. *Updates to the CarbonBond Chemical Mechanism: CB05*; Final Report to the US EPA, RT-0400675; US EPA: Washington, DC, USA, 2005; Available online: http://www.camx.com/publ/pdfs/CB05_Final_Report_12_0805.pdf (accessed on 2 March 2021).
50. Boylan, J.W.; Russell, A.G. PM and light extinction model performance metrics, goals, and criteria for three-dimensional air quality models. *Atmos. Environ.* **2006**, *40*, 4946–4959. [CrossRef]
51. United States Environmental Protection Agency (USEPA). *Guidance on the Use of Models and Other Analyses for Demonstrating Attainment of Air Quality Goals for Ozone, PM_{2.5}, and Regional Haze*; Publication No. EPA-454/B-07-002 April; Office of Air Quality Planning and Standards Air Quality Analysis Division: Research Triangle Park, NC, USA, 2007.
52. Henneman, L.R.F.; Liu, C.; Hu, Y.; Mulholland, J.A.; Russell, A.G. Air quality modeling for accountability research: Operational, dynamic, and diagnostic evaluation. *Atmos. Environ.* **2017**, *166*, 551–565. [CrossRef]
53. Eyth, A.; Pouliot, G.; Vukovich, J.; Strum, M.; Dolwick, P.; Allen, C.; Beidler, J.; Baek, B.H. Development of 2011 Hemispheric Emissions for CMAQ. Presented at the 2016 CMAS Conference, Chapel Hill, NC, USA, 24–26 October 2016; Available online: https://www.cmascenter.org/conference//2016/slides/eyth_development_hemispheric_2016.pptx (accessed on 4 May 2020).
54. Tsai, Y.I.; Chen, C.L. Atmospheric aerosol composition and source apportionments to aerosol in southern Taiwan. *Atmos. Environ.* **2006**, *40*, 4751–4763. [CrossRef]
55. Chou, C.C.K.; Lee, C.T.; Cheng, M.T.; Yuan, C.S.; Chen, S.J.; Wu, Y.L.; Hsu, W.C.; Lung, S.C.; Hsu, S.C.; Lin, C.Y.; et al. Seasonal variation and spatial distribution of carbonaceous aerosols in Taiwan. *Atmos. Chem. Phys.* **2010**, *10*, 9563–9578. [CrossRef]